J Mater Sci: Mater Electron (2021) 32:1379–1391

Investigation of neodymium rare earth element doping in spray-coated zinc oxide thin films

Erman Erdoğan[1,2,*], Mehmet Yilmaz[3,4], Sakir Aydogan[3,5], and Güven Turgut[6]

[1] *Department of Electrical & Electronics Engineering, Muş Alparslan University, Engineering & Architecture Faculty, 49250 Muş, Turkey*
[2] *Electronic Communication Technology Program, Vocational High School, Bilecik Seyh Edebali University, 11230 Bilecik, Turkey*
[3] *Advanced Materials Research Laboratory, Department of Nanoscience and Nanoengineering, Graduate School of Natural and Applied Sciences, Ataturk University, 25240 Erzurum, Turkey*
[4] *Department of Science Teaching, K.K. Education Faculty, Ataturk University, 25240 Erzurum, Turkey*
[5] *Department of Physics, Science Faculty, Atatürk University, 25240 Erzurum, Turkey*
[6] *Department of Basic Sciences, Science Faculty, Erzurum Technical University, 25240 Erzurum, Turkey*

Received: 18 August 2020
Accepted: 16 November 2020
Published online: 2 January 2021

ABSTRACT

In recent years, ZnO films are among the preferred transparent conductive oxides because of their advantageous properties such as being nontoxic, low cost and abundant in nature. In this study, undoped and Nd doped ZnO films were produced on microscope glass substrates with the spray pyrolysis technique, which is an economical and easily applicable method, at a substrate temperature of 380 °C. From the X-ray diffraction patterns, the crystal structures of all films have a preferential orientation (002). It is observed from the XRD peak intensities that the ZnO film with a 3% Nd doping has a (100) preferential orientation. The increase in Nd dopant concentration is the reason for changing the preferred direction of the grains completely. The average particle sizes of the films were calculated using Scherrer and Williamson–Hall method. It was determined that the film with 2% Nd doped crystallized better than other films and the largest particle size belongs to this film. The transmittance spectra of Nd doped ZnO films were taken using a UV–Vis spectrophotometer. The optical transmittance spectrum of the films shows that in the visible region, all films have a value of over 90%. Optical band gap values were calculated using these spectra. According to the results obtained, it was determined that the optical band value of the ZnO film decreased first with the Nd contribution, and started to increase when the amount of dopant increased. The surface morphology of the films was analyzed by optical profilometer and surface roughness values were determined. It indicates that the films grown on the glass substrate, as observed in the XRD analysis of the films, consist of nanoscale particles. It has been observed that the surface roughness of the films varies with the increasing

Address correspondence to E-mail: e.erdogan@alparslan.edu.tr; erman0702@gmail.com

https://doi.org/10.1007/s10854-020-04907-1

amount of Nd. To investigate the surface conditions of the films, the scanned electron microscopy (SEM) images of the obtained films were taken. From the SEM images, it was observed that the surfaces of the films were similar to each other, were nonporous and homogeneous. With this study, the effect of Nd doping on structural, optical and superficial properties of ZnO films was investigated and it was determined that Nd doping of ZnO films were suitable materials for optoelectronic applications.

1 Introduction

Semiconductor materials form the basis of electronics. The developing and changing world has caused different needs to emerge every day. Especially in recent years, studies on semiconductor technology have gained speed [1]. Zinc oxide (ZnO), one of the most used nanostructured materials in semiconductor technology, has a wide optical conductivity and high electrical conductivity at room temperature of about 3.37 eV. Besides, this semiconductor has high transmittance in the visible region [2]. It is of great importance for nano-devices in terms of morphological, mechanical, electronic, optical, and structural features. Especially Al doped ZnO nanorods can be used as a leg of a nanogenerator for thermoelectric energy harvesting [3]. ZnO semiconductor thin films are an important material used in many scientific types of researches because of their low cost, nontoxic, environmentally friendly and can be easily doped with different elements [4]. They are used in the structure of many electronic circuit elements such as thin film transistors, high power electronic circuits, light emitting diodes (LED), field effect transistors (FET), sensors, solar cells [5–10]. Since the crystal structure of ZnO is hexagonal wurtzite, its electrical, morphological, and optical properties can be changed by heat treatments or various dopants. Because of these important properties, zinc oxide thin films are generally preferred.

ZnO thin films are obtained with a wide range of deposition techniques; such as, chemical vapor deposition (CVD), pulsed laser deposition (PLD), sol–gel spin coating, hydrothermal synthesis, magnetron sputtering and electrodeposition [11–16]. Compared with these methods, the spray coating method is the easiest and cheapest method of obtaining a thin film. The advantages of the spraying method are also enormous. Among them, it is quite simple, it is more economical in terms of necessary equipment, it is suitable for intervention in the production process, there is no need for vacuum media for thin film production and the production process can be followed step by step [17]. This method allows for n-type and p-type dopants. The quality of the film may vary with some parameters; such as substrate temperature, spraying ratio and film thickness. Experimental parameters such as the spray nozzle diameter, the nozzle lower base distance, and the pure water ratio are also important in obtaining a good film. The droplet size of the sprayed solution plays a big role in the quality of the film [18]. It is possible to come across produced ZnO thin films using the spray technique in the literature. The general purpose of these studies is to investigate the physical properties of the obtained ZnO thin films [19–23].

When studies conducted in recent years are examined, ZnO films are doped with many elements and their physical properties are investigated. Having a wide range of optical bands, ZnO becomes a suitable material for optoelectronic devices if it is doped with elements called rare earth (RE) elements. When ZnO is doped with rare earth ions, it not only allows the absorption of high energy photons gap, but also allows a more efficient energy transfer to rare earth ions [24]. ZnO doped with rare earth metals (Pr, Eu, Sm and La) with spray technique are impressive materials due to their ability to change some physical properties [25–28]. RE elements placed in ZnO films can modulate the surface structure and induce the change of optical properties such as band gap and transmittance. Also, RE elements are suitable as doping materials owing to their electronic transitions and high conductivity occurring in 4f energy shells [29]. Particularly, films containing Nd ions are a good candidate for optoelectronic devices because of the playing carrier donors and energy transfer [30]. Nd^{3+} has an ionic radius of 0.108 nm which is slightly more than the host Zn^{2+} radius of 0.083 nm. Nd doped

ZnO leads to a band gap narrowing although the dopant is in + 3 states [31].

When compared with some physical properties of Nd-doped ZnO thin films obtained in vacuum-requiring environments, which are summarized in Table 1, obtaining similar results by using a simple, cheap, useful method that does not require a vacuum environment reveals the importance of this study.

In this study, undoped and Nd doped ZnO thin films have been deposited on glass substrates with the spray pyrolysis technique. We aim to produce films that can be used in some optoelectronic devices and especially semiconductor thin film solar cells by using the spray pyrolysis technique and to examine the effect of Nd contribution to the optical, surface, and structural properties of films.

2 Experimental

2.1 Substrate cleaning

In order for the film to be obtained to be homogeneous and good physical properties, the substrates must be clean. Therefore, one of the most important steps in film production is the cleaning of the substrate to be used. In this study, microscope glass substrates were cut to ~ 1 cm × 1 cm with the help of a diamond cutter. Firstly, glass substrates were washed with deionized (DI) water for 20 min at 60 °C with an ultrasonic mixer to remove impurities on the substrates. Substrates extracted from DI water were immersed in methanol and acetone and washed at 60 °C for 20 min with an ultrasonic mixer. The glasses rinsed with DI water were finally dried in an oven at 100 °C for 1 h. Thus, the glasses are ready for use for experiments. The production of the film on the cleaned plaster was made immediately without waiting.

2.2 Preparation of the solutions

As-deposited and Nd doped ZnO films (% wt 1, 2, 3) were produced on microscope glass substrates at 380 °C temperature using the spray pyrolysis technique. [Zinc acetate Zn $(CH_3COO)_2{\cdot}2H_2O$] (Merck) chemical salt was used as the source of Zn and O. Starting solution was prepared at a concentration of 0.3 M. As the Nd source, the neodymium (III) nitrate hexahydrate [Nd $(CH_3COO)_2{\cdot}6H_2O$] (Sigma Aldrich) with 99.99% purity was used. Five different solutions were prepared depending on the Nd dopant. Then, the solution mixtures were subjected to constant stirring for 15 min at room temperature to produce a homogeneous and clear solution and it was used as a source for spray technique.

2.3 Obtaining thin films

The prepared substrates and solutions were placed in the chemical spray system. The distance between the tip of the ultrasonic atomizer and the samples was adjusted to be 30 cm. The controller was programmed to cool to 25 °C after going up to 380 °C for 60 min and waiting for 60 min for 380 °C. When the temperature of the substrate was 380 °C, the sample holder started to be rotated at a constant speed to obtain homogeneous samples. The power supply of the ultrasonic atomizer was operated at a frequency of 100 MHz and the atomizer was also pressed into 70 bar of dry air.

Table 1 Comparison of some parameters obtained vacuum-deposited Nd-doped ZnO thin films to our work

	Deposition technique	Crystallite size (nm)	Optical band gap (eV)	Average optical transmittance (%)	References
Nd doped ZnO	Pulsed electron beam	12–13	3.27–3.30	–	Nistor et al. [32]
Nd doped ZnO	RF magnetron sputtering	11–26	–	–	Huang et al. [33]
Nd doped ZnO	Pulsed laser	–	3.26–3.47	90 (visible)	Nistor et al. [34]
Nd doped ZnO	Spray pyrolysis	18–40	3.28–3.32	90–95 (transparent)	In this work

2.4 Characterization

The surface morphologies of the undoped and Nd doped ZnO films were studied using the Quanta FEG 250 scanning electron microscope (SEM). SEM images were taken under 1.00 or 2.00 kV voltage to prevent damage to the film surfaces. X-ray diffraction (XRD) spectra of the films were taken using the EXPLORER XRD device at 2θ = 20°–80° in 0.02° steps, at 15 rpm sample holder rotation speed. XRD measurements were performed with monochromatic CuKα (λ = 1.54059 Å) beam. In addition to supporting SEM images, optical profilometer analyzes (Contour GT, Bruker) were also obtained to get more detailed information about the surface morphology of the studied samples. Optical properties were evaluated by UV–Vis spectrophotometer (Shimadzu UV-3600 Plus) in the wavelength range of 200–1000 nm. All characterization measurement were taken at Erzurum Technical University High Technology Research and Application Center (ETU-YUTAM).

3 Results and discussions

3.1 XRD investigations

In the XRD method, X-ray analysis is carried out through the substance. The intensities and widths of the peaks are examined from the X-ray diffraction patterns to determine whether the films crystallize well or poorly. High-density sharp peaks in the XRD spectrum of a sample indicate low FWHM values indicating high crystallinity, while the opposite indicates low crystallization. For Nd doped and pure ZnO thin films, X-ray diffraction patterns were measured in the EXPLORER X-ray diffractometer using a CuKα beam with a wavelength of λ = 0.154 nm. In Fig. 1, the X-ray diffraction pattern of pure, 1%, 2% and 3% Nd added ZnO films are given. In the diffraction patterns, six peaks generally originating from the planes (100), (002), (101), (102), (103) and (112) were observed. This shows that the films have a poly-crystal structure.

Since the doping level is very low, no peaks of Nd_2O_3 and $Nd(OH)_3$ phases related to Nd dopant are observed. The highest peak is seen in pure ZnO thin film. Besides, the preferred orientation for pure, 1% and 2% Nd doped ZnO films is the plane with the highest peak intensity (002). The pure ZnO thin film has a high preferential orientation along the (002) plane. This shows that the pure ZnO thin film exhibits a strong c-axis orientation perpendicular to the substrate [35]. The preferred orientation for the ZnO thin film with 3% Nd doping is the plane (100). This shows that some grains grow in other orientations besides the c-axis orientation [36]. Also, observing the peaks of (100), (002), (101), (102), (103) and (112) at different intensities indicates that growth is anisotropic for all films.

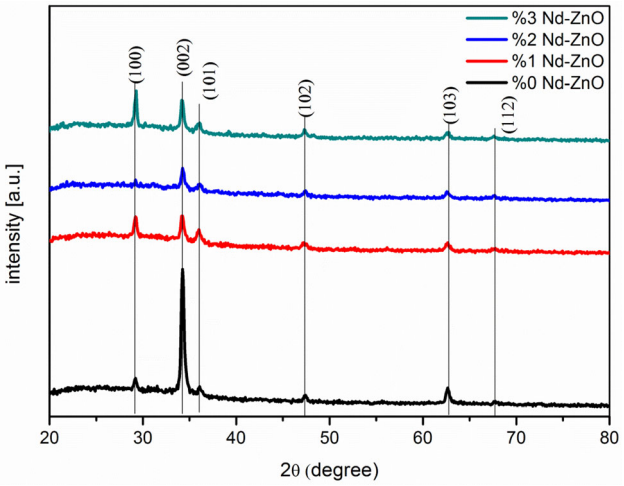

Fig. 1 XRD diffraction pattern of pure and Nd doped ZnO thin films

In the diffraction pattern of the 3% Nd-doped ZnO thin film, the increase in the intensity of the peaks of the (100) and (110) planes, and the decrease in the intensity of the diffraction peak of the (002) plane can be seen as an important result. This result points out that the thin film grains grow parallel to the substrate surface. Nd doping causes a decrease in the crystallinity of ZnO thin films [37].

By using the equation of 2θ values of plane peaks in the X-ray diffraction pattern of pure and doped ZnO films, the distance between the planes of the hexagonal wurtzite structure (d_{hkl}) was calculated following formula [38]:

$$n\lambda = 2\,d_{hkl}\sin\theta. \tag{1}$$

To get detailed information about the crystal structure, the crystal dimensions D of all planes were determined using the modified plot based on the following formula [39]:

$$\ln\beta = \ln\frac{0.9\lambda}{D} + \ln\frac{1}{\cos\theta}, \tag{2}$$

where "D" is the estimated crystal size, "λ" is the wavelength (1.5418 Å) of the incoming X-ray, β is the full width half maximum (FWHM) value in radians and the θ is the Bragg angle of the diffraction peaks. If we draw the results of ln β according to ln (1cos θ), a straight line with an approximate slope and an intersection of ln $0.9/D$ should be obtained. Therefore, a single value of D in the nanometer scale can be calculated. According to the calculated average crystal size values of the samples determined from the intercept of the plot given in Fig. 2, it was concluded that the crystal size varied with increasing Nd amount. Calculated average crystal sizes of the pure and 1%, 2% and 3% Nd doped ZnO films were found as 24.57 nm, 18.85 nm, 40.07 nm and 29.29 nm, respectively. Since the ionic radius of Nd (0.136 nm) is very close to the ionic radius of oxygen (0.132 nm), it can be said that Nd in the ZnO crystal structure tends to be replaced by oxygen. Therefore, we can say that we observed such a difference in the size of the crystal with the Nd content [40, 41].

Using the Williamson–Hall method, crystal size and lattice tension can be calculated for each sample and their changes can be examined depending on the rate of contribution. Williamson–Hall method is a method developed considering that particle size and micro strain effects are the two biggest factors affecting the peak width [42]. Crystalline size, lattice errors, and instrumental peak width determine the total peak width measured. Strain-induced broadening due to crystal imperfections and deformity are dependent on the tan θ in W–H analysis Strain-induced peak expansions fall under the category of errors in the crystal and strain can be calculated following formula [43]:

$$\varepsilon = \frac{\beta_s}{4\tan\theta}, \tag{3}$$

where β_s is the FWHM of the strain broadening. Scherrer equation and the equation given above create the following equations:

$$\beta_D{}^2 = \beta_{measured}{}^2 - \beta_{instrumental}{}^2, \tag{4}$$

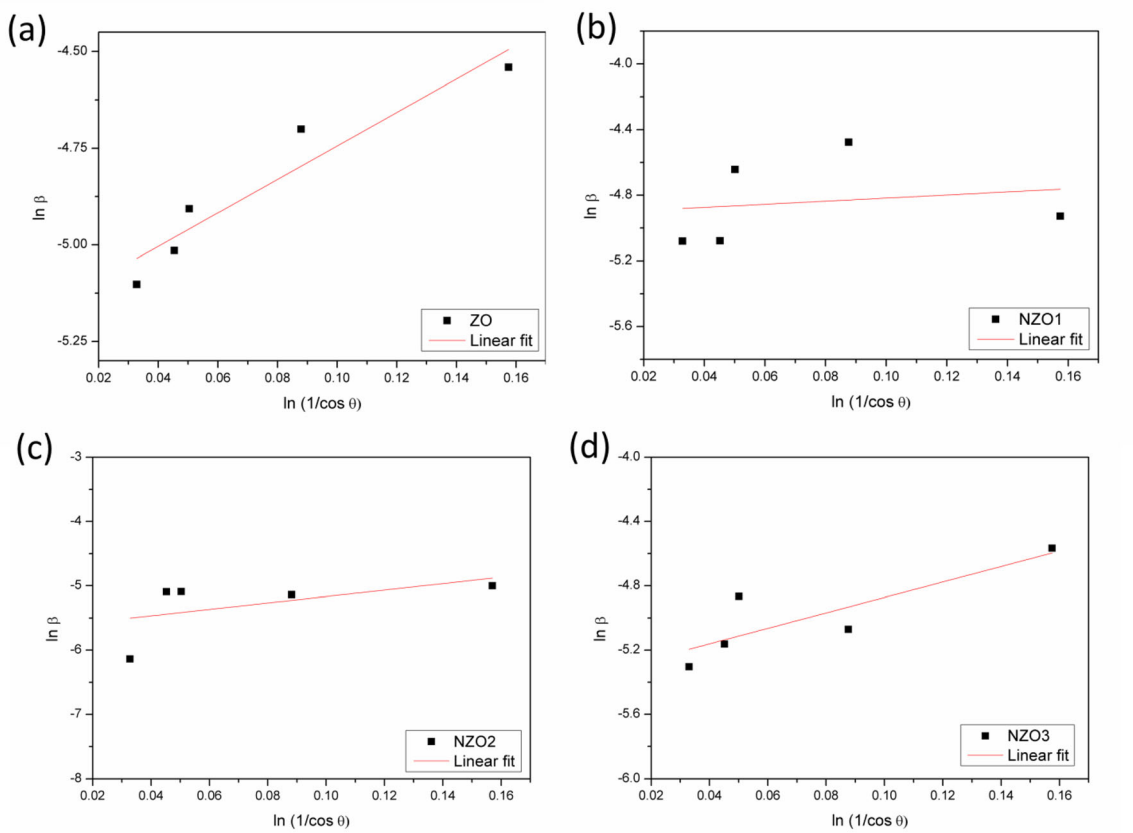

Fig. 2 Modified Scherrer plots of pure and Nd doped ZnO thin films

$$D = \frac{K\lambda}{\beta_D \cos\theta} \rightarrow \cos\theta \frac{K\lambda}{D}\left(\frac{1}{\beta_D}\right), \tag{5}$$

where β_D is the FWHM of the peak broadening, K is the shape factor, D is the crystallite size and λ is the wavelength of the CuK_α radiation. Taking above equations into consideration:

$$\beta_{hkl} = \beta_s - \beta_D, \tag{6}$$

$$\beta_{hkl} = \left(\frac{k\lambda}{D\cos\theta}\right) + (4\varepsilon\tan\theta), \tag{7}$$

$$\beta_{hkl}\cos\theta = \left(\frac{k\lambda}{D}\right) + (4\varepsilon\sin\theta). \tag{8}$$

Accordingly, the sum of these two factors is associated with peak expansion, and a new equation is created. Given equations are known as the Williamson–Hall equations [44]. According to these equations, strains are assumed to be equal in all crystallographic directions. When the values in the drawn plot are fit, the curve of the line plot that crosses the y-axis of the plot gives the crystalline size [45]. Their variations and the values of D, ε are calculated using the modified Scherrer method and W–H analysis for pure and Nd doped ZnO films and given in Table 2. Furthermore, the values of (hkl), 2θ and β_{hkl} used for the modified Scherrer method and W–H method are also summarized in Table 2.

As seen in Fig. 3, the plotted graph indicates that pure and Nd-doped ZnO samples exhibit a positive gradient which represents the positive strain in the samples. Calculated average crystal sizes of the pure and 1%, 2% and 3% Nd doped ZnO films were found as 46.69 nm, 20.21 nm, 61.64 nm and 65.41 nm, respectively. Considering the XRD measurements, it can be said that the film quality varies with the addition of Nd as the strain value appears at different values in the ZnO structure.

3.2 Optical investigations

Reflection, transmittance and absorption spectra of thin films are obtained with UV–Vis spectroscopy. UV–Vis spectroscopy is important because it provides the electronic properties of thin film and the development of films used in application areas. It is

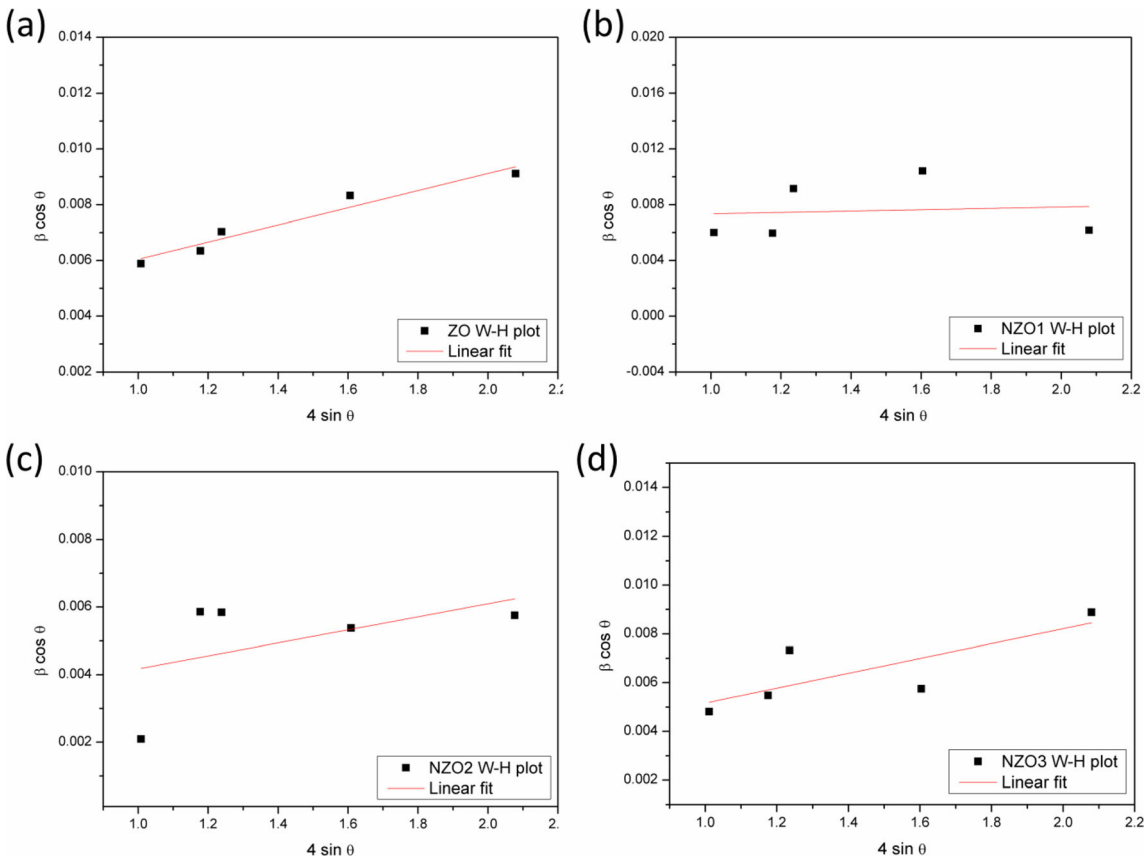

Fig. 3 Williamson–Hall (W–H) plots of pure and Nd doped ZnO thin films

Table 2 Comparison of some structural parameters of ZnO:Nd thin films (d_{hkl}: interplanar distance, *FWHM* full width half maximum, $D_{SR\text{-}ort}$ crystal size from modified Scherrer plot, $D_{W\text{-}H\text{-}ort}$ crystal size from W–H plot, ε_{SR} microstrain from modified Scherrer plot, $\varepsilon_{W\text{–}H}$ microstrain from W–H plot

	(*hkl*)	d_{hkl} (Å)	2θ (°)	FWHM (°)	$D_{\text{SR-ort}}$ (nm)	$D_{\text{W–H-ort}}$ (nm)	ε_{SR} ($\times 10^{-3}$)	$\varepsilon_{\text{W–H}}$ ($\times 10^{-3}$)
ZnO:Nd %0	(100)	3.057723	29.19	0.3485	24.57	46.69	1.834	3.080
	(002)	2.615937	34.26	0.3803				
	(101)	2.488045	36.08	0.4237				
	(102)	1.918823	47.35	0.5208				
	(103)	1.482251	62.64	0.6110				
ZnO:Nd %1	(100)	3.056698	29.20	0.3562	18.85	20.21	1.885	0.482
	(002)	2.621132	34.19	0.3571				
	(101)	2.494060	35.99	0.5511				
	(102)	1.921501	47.28	0.6514				
	(103)	1.482464	62.63	0.4147				
ZnO:Nd %2	(100)	3.056698	29.20	0.3562	40.07	61.64	1.245	1.920
	(002)	2.617419	34.24	0.3571				
	(101)	2.488712	36.07	0.5511				
	(102)	1.915773	47.43	0.6514				
	(103)	1.484168	62.55	0.4147				
ZnO:Nd %3	(100)	3.0485285	29.28	0.2849	29.29	65.41	1.612	3.050
	(002)	2.6218763	34.18	0.3282				
	(101)	2.4940602	35.99	0.4413				
	(102)	1.9218838	47.27	0.3597				
	(103)	1.4822514	62.64	0.5956				

also one of the methods often used to determine the optical energy band gap of a semiconductor.

Optical transmittance was measured in the wavelength range of 200–1000 nm to get information about the effect of the neodymium dopant amount on the optical properties of ZnO films. At large wavelengths ($\lambda > 400$) all films are transparent and there is no scattering or absorption of light. Short wavelengths ($\lambda < 400$) are known as absorption zone due to the presence of absorption. In the transparent region, the average % transmittance was found to be 94.49, 90.83, 92.24 and 95.49 for ZnO films with 0%, 1%, 2% and 3% Nd dopants, respectively. All Nd doped ZnO films show a sharp absorption edge around 355 nm in the UV region due to the initial basic absorption. The observation of the sharp absorption band for the film NZO means that films are favorable for photovoltaic applications [46]. Additionally, sharp absorption edges relating to the electron's excitation from the conductance band to the valence band are visible in the spectra as given in Fig. 4.

Compared with the pure ZnO film, the probable reason for increasing optical transmittance in ZnO film starting with a 2% Nd dopant can be shown to be occupied by Nd in the spaces found in ZnO. This reduces the scattering of light in the structure and causes increased transmittance. All the above-mentioned results are compatible with the structural and morphological features of the films presented in this study. To look into the Nd impurities in the structure and the optical band gap changes, the optical band

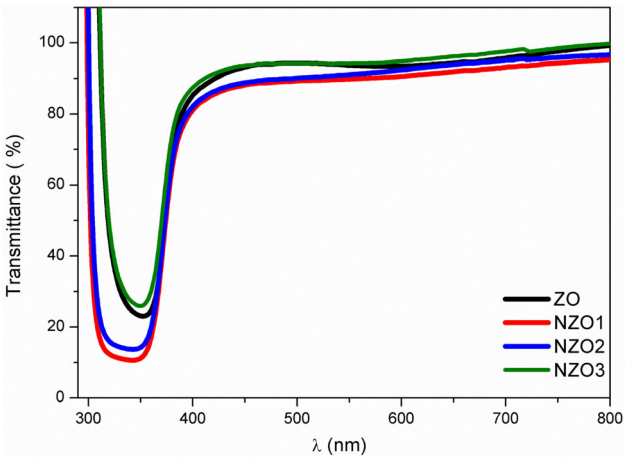

Fig. 4 Optical transmittance spectra of the ZnO films with various Nd content

gap of the films was calculated by the following equation:

$$(\alpha hv)^2 = C(hv - E_g).$$

Here, "α" is the absorption coefficient, C is a constant value and the hv is the energy of a photon. The direct band gap of the films is obtained with the fit applied on the energy axis of the linear part of the (hv) graphic against $(\alpha hv)^2$. Calculated E_g values are in the range of 3.28–3.32 eV as given in Fig. 5. Deepa Rani and co-workers have found that the bandgap values are diverse between 3.20 and 3.22 eV with the increase in Nd doping from 0 to 0.25% [47].

Based on the obtained results, it is procured that the E_g values show the rising inclination with increasing Nd content as well as some undulations are seen in Fig. 5. Resembling results have been found by the literature for La doped ZnO films which can be explained as a possible result of the Burstein–Moss effect [48]. The states of the current energy in the optical band gap of ZnO films with Nd doping affect the structure of the manner of the optical transition and optical band gap.

3.3 Optical profilometer investigations

An optical profilometer is a technique of connecting light from multiple sources in an optical device to make diverse exact measurements. This method has been carried out to characterize surface roughness, surface profile, and surface topography. Images and surface roughness of all samples were obtained using an optical profilometer (Contour GT, Bruker), which can analyze on a relatively large surface area and provide the fast and contactless mapping of the surface in three dimensions. Figure 6 shows the 2D and 3D morphological profiles of the pure and Nd doped ZnO samples fulfilled by optical profilometry including the average roughness values taken from regions across each sample.

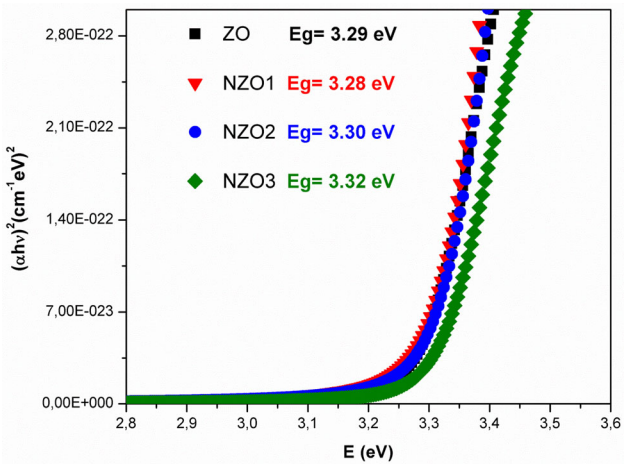

Fig. 5 Variation of optical band gap of ZnO films with Nd content

When the images are analyzed, red regions are seen in some areas of the film, which are formed as a result of the accumulation and clustering of grains of different widths and heights, and which become more apparent with the increasing amount of Nd. However, it is observed that the effect of the blue regions which indicates that the accumulation is less on the surface and is also the symptom of the pure ZnO film also continues with the increasing amount of Nd.

It is seen that all the synthesized films have a polycrystalline structure with a homogeneous distribution of the particles. Also, it indicates that the films grown on the glass substrate, as observed in the XRD analysis of the films, consist of nanoscale particles. It has been monitoring that the surface roughness of the films varies with the increasing amount of Nd. The average surface roughnesses (R_a) for ZnO films with 0%, 1%, 2% and 3% Nd dopants were found as 54.86, 55.08, 53.18 and 46.61 nm, respectively. Similarly, root mean square roughness (R_q) for ZnO films with 0%, 1%, 2% and 3% Nd dopants was found as 86.28, 82.55, 74.77, and 77.26 nm, respectively. It is concluded that the obtained values are very close to each other. Taking into account the growth manner of the films, it can be concluded that the diffusion of the crystal surface-bound atoms between adjacent crystal particles varies slightly with the amount of neodymium, thereby producing films with close surface roughness. Prasada Rao et al. have examined the AFM images of pure and Nd doped ZnO films using the spray technique. They reported the average surface roughness values of pure and Nd doped ZnO films as 28.1 nm and 46.3 nm, respectively. It is seen that these values are smaller than those of the values in our study [49].

3.4 SEM investigations

Scanning electron microscopy (SEM) was used to obtain high-resolution surface topography of the samples. The surface morphologies of the films were studied using the Quanta FEG 250 scanning electron microscope (SEM). From SEM images, it can be

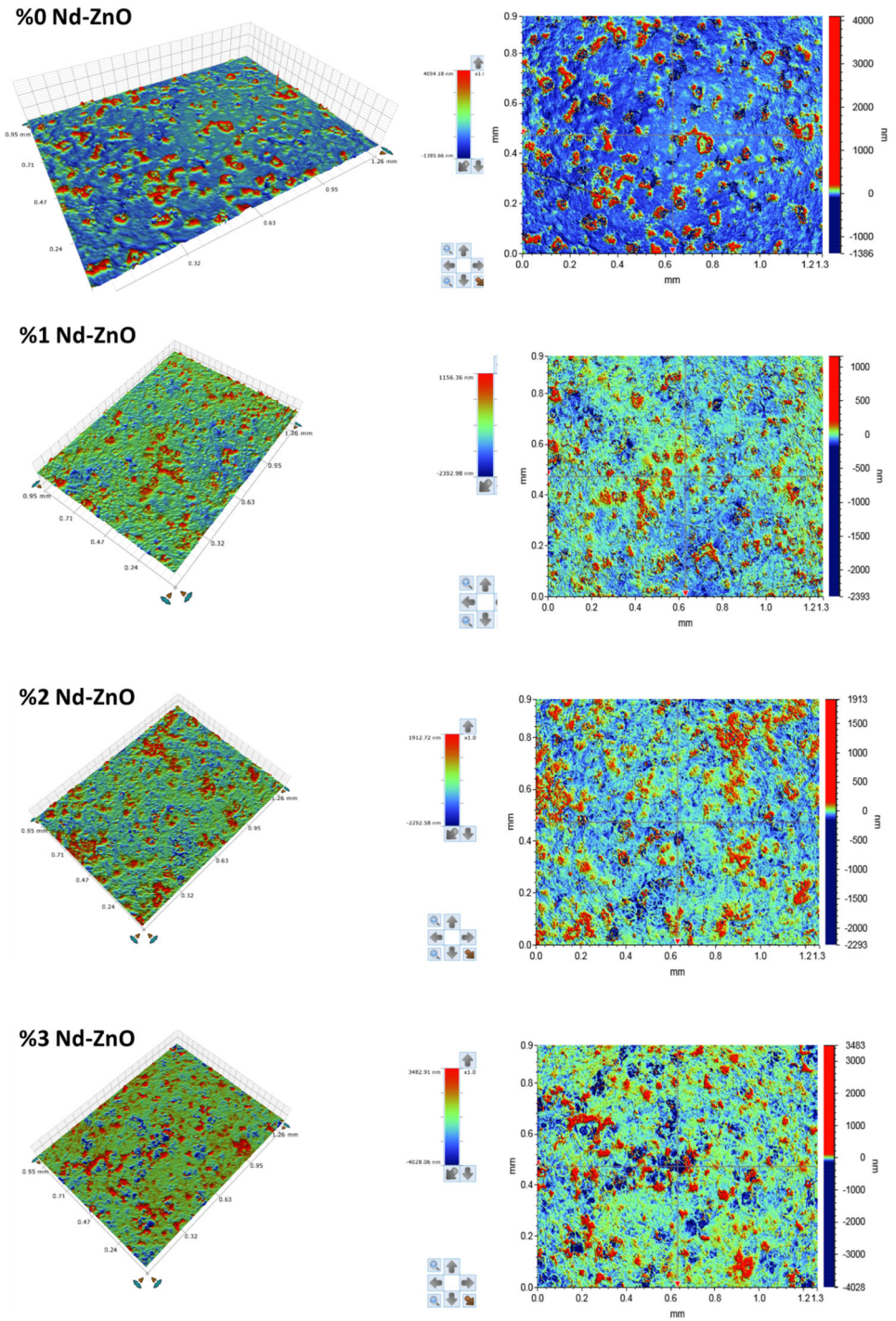

Fig. 6 2D and 3D optical profilometer images of pure and Nd doped ZnO thin films

concluded that all films consist of uniform and dense ZnO particles. When the SEM images of the films obtained are examined (Fig. 7), it is seen that the film surfaces are formed in a smooth and homogeneous continuous structure without cracks, spaces and pores, and the glass substrates are well coated. The particles were formed as a mixture of columnar and granular microstructures, coherent with AFM results. From SEM images, changes in crystal size with Nd doping were observed. It can be inferred that the surface morphology of the films sorely is contingent on the dopant concentration [50].

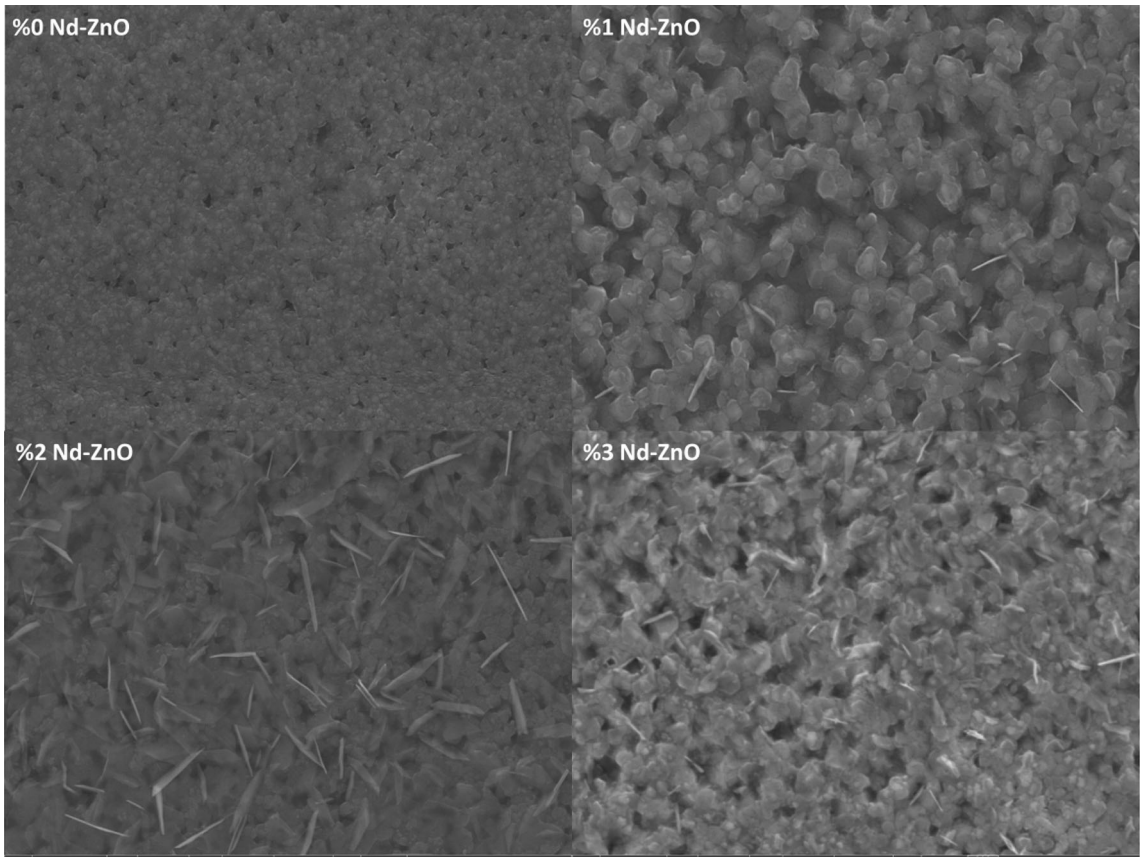

Fig. 7 SEM images of pure and Nd doped ZnO thin films

4 Conclusion

Transparent conductive oxide semiconductor films have been studied intensively in recent years due to their appropriate physical properties and have attracted a lot of attention. ZnO and ZnO:Nd (1%, 2%, 3%, and 4%) are synthesized using the spray pyrolysis technique. In this study, the contribution of the Nd element in different ratios was chosen as the test parameter and it was seen that this production parameter had a significant impact on the formation of films and some physical properties. The structural, optical, morphological and superficial properties of films were searched with XRD, UV–Vis, SEM and Optical profilometer methods. From XRD patterns it is seen that the orientation of ZnO film is changed from (002) to (100) plane and the crystalline size varied with Nd doping. The grain sizes of films obtained from the modified Scherrer Method were smaller than the grain sizes obtained from W–H Analysis. This difference is proportional to the strain value and indicates that the strain plays an important role. Therefore instrument broadening must be taken into account for calculating the grain size. It was observed from the optical spectroscopy measurements, the average % transmittance was found to be 94.49, 90.83, 92.24, and 95.49 for ZnO films with 0%, 1%, 2% and 3% Nd dopants, respectively in the transparent region. Although the optical band gaps calculated using the transmittance spectra are almost the same, it is determined that ZnO film with 3% Nd dopant has the widest band gap compared to other films. It was observed from the optical profilometer images to determine the superficial properties of ZnO:Nd films that different grains with different widths and heights were formed on the surfaces of all films. In addition, it was determined that ZnO films with 3% Nd dopants have the lowest roughness values among all films. From the SEM images, it is seen that the ZnO structure is homogeneously coated on the substrate, there are no agglomerate formations and there are no gaps on the surface, so that the grains are held together better and Nd structures appear to be occasionally located on the surface with

the increasing amount of dopants. The neodymium-doped ZnO film produced by the spray pyrolysis technique can be used for optoelectronic applications.

Funding

The author(s) received no specific funding for this work.

Data availability

Authors can confirm that all relevant data are included in the article.

Compliance with ethical standards

Conflict of interest The authors declare that there is no conflict of interest.

References

1. D.P. Kumah, J.H. Ngai, L. Kornblum, Epitaxial oxides on semiconductors: from fundamentals to new devices. Adv. Func. Mater. **30**(18), 1901597 (2020)
2. J. Theerthagiri, S. Salla, R.A. Senthil, P. Nithyadharseni, A. Madankumar, P. Arunachalam, T. Maiyalagan, H.S. Kim, A review on ZnO nanostructured materials: energy, environmental and biological applications. Nanotechnology **30**(39), 392001 (2019)
3. M. Norouzi, M. Kolahdouz, P. Ebrahimi, M. Ganjian, R. Soleimanzadeh, K. Narimani, H. Radamson, Thermoelectric energy harvesting using array of vertically aligned Al-doped ZnO nanorods. Thin Solid Films **619**, 41–47 (2016)
4. M. Samadi, M. Zirak, A. Naseri, E. Khorashadizade, A.Z. Moshfegh, Recent progress on doped ZnO nanostructures for visible-light photocatalysis. Thin Solid Films **605**, 2–19 (2016)
5. G.R. Yi, H.S. Kim, D.H. Lee, B. Kim, C.K. Kim, Effect of annealing on performance of ZnO thin film transistors. Mol. Cryst. Liq. Cryst. **678**(1), 43–52 (2019)
6. M. Benlamri, B.D. Wiltshire, Y. Zhang, N. Mahdi, K. Shankar, D.W. Barlage, High breakdown strength Schottky diodes made from electrodeposited ZnO for power electronics applications. ACS Appl. Electron. Mater. **1**(1), 13–17 (2019)
7. F. Rahman, Zinc oxide light-emitting diodes: a review. Opt. Eng. **58**(1), 010901 (2019)
8. Y. Kim, M. Chang, S. Cho, M. Kim, H. Kim, E. Choi, E. Ko, J. Hwang, B. Park, Formation of a functional homo-junction interface through ZnO atomic layer passivation: enhancement of carrier mobility and threshold voltage in a ZnO nanocrystal field effect transistor. J. Alloys Compd. **804**, 213–219 (2019)
9. D. Thomas, J. Prakash, K.K. Sadasivuni, K. Deshmukh, A.J. Edakkara, Surface modified zinc oxide nanoparticles as smart UV sensors. J. Electron. Mater. **48**(7), 4726–4732 (2019)
10. J. Luo, Y. Wang, Q. Zhang, Progress in perovskite solar cells based on ZnO nanostructures. Sol. Energy **163**, 289–306 (2018)
11. T. Saito, R. Iba, S. Ono, G. Imada, K. Yasui, Growth characteristics of ZnO thin films produced via catalytic reaction-assisted chemical vapor deposition. J. Vac. Sci. Tech A **37**(3), 030904 (2019)
12. V. Kumar, S.K. Singh, H. Sharma, S. Kumar, M.K. Banerjee, A. Vij, Investigation of structural and optical properties of ZnO thin films of different thickness grown by pulsed laser deposition method. Physica B **552**, 221–226 (2019)
13. A. Tab, A. Abderrahmane, Y. Bakha, S. Hamzaoui, M. Zerdali, Investigation on the optical transmission in UV range of sol-gel spin coated zinc oxide nanofilms deposited on glass. Optik **194**, 163073 (2019)
14. L. Zhu, Y. Li, W. Zeng, Hydrothermal synthesis of hierarchical flower-like ZnO nanostructure and its enhanced ethanol gas-sensing properties. Appl. Surf. Sci. **427**, 281–287 (2018)
15. M.A. Cruz, O. Ceballos-Sanchez, E. Luévano-Hipólito, L.M. Torres-Martínez, ZnO thin films deposited by RF magnetron sputtering: effects of the annealing and atmosphere conditions on the photocatalytic hydrogen production. J. Hydrogen Energy **43**(22), 10301–10310 (2018)
16. F. Caballero-Briones, J.A. Barón-Miranda, C. Guarneros-Aguilar, O. Calzadilla, F. Sanz, Influence of pulse frequency on the morphology, structure and optical properties of ZnO films prepared by pulsed electrodeposition. Mater. Res. Exp. **6**(8), 086464 (2019)
17. D. Perednis, L.J. Gauckler, Thin film deposition using spray pyrolysis. J. Electrocer. **14**(2), 103–111 (2005)
18. S.R. Ardekani, A.S.R. Aghdam, M. Nazari, A. Bayat, E. Yazdani, E. Saievar-Iranizad, A comprehensive review on ultrasonic spray pyrolysis technique: mechanism, main parameters and applications in condensed matter. J. Analy. Appl. Pyrol. **141**, 104631 (2019)
19. M. Acosta-Osorno, S. Alcántara-Iniesta, J. Alvarado, C.D. Young, I. Mejía, M. García, J.R. Ramos-Serrano, G. Juarez-Díaz, Characterization of ZnO thin films obtained by ultrasonic spray pyrolysis for application in UV photoconductive detectors. Mater. Res. Exp. **6**(11), 116450 (2019)

20. E. Muchuweni, T.S. Sathiaraj, H. Nyakotyo, Synthesis and characterization of zinc oxide thin films for optoelectronic applications. Heliyon **3**(4), e00285 (2017)
21. A.A. Rani, S. Ernest, Characterization of spray-deposited ZnO thin films for dye-sensitized solar cell application. Appl. Phys. A **122**(7), 647 (2016)
22. V.P. Deshpande, S.D. Sartale, A.N.A.U. Ubale, Temperature dependent properties of spray deposited nanostructured ZnO thin films. Int J Mater Chem **7**(2), 36–46 (2017)
23. Ş Aydoğan, M.L. Grilli, M. Yilmaz, Z. Çaldiran, H. Kaçuş, A facile growth of spray based ZnO films and device performance investigation for Schottky diodes: determination of interface state density distribution. J. Alloys Compd. **708**, 55–66 (2017)
24. R. Röder, S. Geburt, M. Zapf, D. Franke, M. Lorke, T. Frauenheim, A. Luisa da Rosa, C. Ronning, Transition metal and rare earth element doped zinc oxide nanowires for optoelectronics. Phys. Status Solidi (b) **256**(4), 1800604 (2019)
25. N. Narayanan, N.K. Deepak, Praseodymium: a competent dopant for luminescent downshifting and photocatalysis in ZnO thin films. Zeitschrift für Naturforschung A **73**(5), 441–452 (2018)
26. R. Swapna, T. SrinivasaReddy, K. Venkateswarlu, M.S. Kumar, Effect of post-annealing on the properties of Eu doped ZnO nano thin films. Proced. Mater. Sci. **10**, 723–729 (2015)
27. P. Velusamy, R.R. Babu, K.T. Aparna, Effect of Sm doping on the physical properties of ZnO thin films deposited by spray pyrolysis technique. AIP Conf. Proceed. **1832**(1), 080085 (2017)
28. M.M. Ahmed, W.Z. Tawfik, M.A.K. Elfayoumi, M. Abdel-Hafiez, S.I. El-Dek, Tailoring the optical and physical properties of La doped ZnO nanostructured thin films. J. Alloys Compd. **791**, 586–592 (2019)
29. A. Hastir, N. Kohli, R.C. Singh, Comparative study on gas sensing properties of rare earth (Tb, Dy and Er) doped ZnO sensor. J. Phys. Chem. Solids **105**, 23–34 (2017)
30. T. Deeparani, K. Ramamurthi, E. Elangovan, G. Salvan, Comparison studies of Nd doped ZnO thin films doped by spray pyrolysis technique. AIP Conf. Proceed. **2115**(3), 030201 (2019)
31. M. Subramanian, P. Thakur, S. Gautam, K.H. Chae, M. Tanemura, T. Hihara, R. Jayavel, Investigations on the structural, optical and electronic properties of Nd doped ZnO thin films. J. Phys. D Appl. Phys. **42**(10), 105410 (2009)
32. M. Nistor, L. Mihut, E. Millon, C. Cachoncinlle, C. Hebert, J. Perriere, Tailored electric and optical properties of Nd doped ZnO: from transparent conducting oxide to photon downshifting thin films. RSC Adv **6**(47), 41465–41472 (2016)
33. Z.Y. Huang, P. Luo, M. Chen, S.R. Pan, D.H. Chen, Microstructure and hemocompatibility of neodymium doped zinc oxide thin films. Mater. Lett. **65**(15–16), 2345–2347 (2011)
34. M. Nistor, E. Millon, C. Cachoncinlle, W. Seiler, N. Jedrecy, C. Hebert, J. Perrière, Transparent conductive Nd-doped ZnO thin films. J. Phys. D Appl. Phys. **48**(19), 195103 (2015)
35. L. Zhao, G.J. Shao, X.J. Qin, Concentration-dependent behavior of hydrogen in Al-doped ZnO thin films. J. Alloys Compd. **509**(30), 297–300 (2011)
36. J. Li, J. Xu, Q. Xu, G. Fang, Preparation and characterization of Al doped ZnO thin films by sol–gel process. J. Alloys and Comp. **542**, 151–156 (2012)
37. K.M. Sandeep, S. Bhat, S.M. Dharmaprakash, Structural, optical, and LED characteristics of ZnO and Al doped ZnO thin films. J. Phys. Chem. Solids **104**, 36–44 (2017)
38. P. Bindu, S. Thomas, Estimation of lattice strain in ZnO nanoparticles: X-ray peak profile analysis. J. Theor. Appl. Phys. **8**(4), 123–134 (2014)
39. A. Monshi, M.R. Foroughi, M.R. Monshi, Modified Scherrer equation to estimate more accurately nano-crystallite size using XRD. World J. Nano Sci. Eng. **2**(3), 154–160 (2012)
40. J. Wu, Y. Zhao, C.Z. Zhao, L. Yang, Q. Lu, Q. Zhang, Y. Zhao, Effects of rapid thermal annealing on the structural, electrical, and optical properties of Zr-doped ZnO thin films grown by atomic layer deposition. Mater. **9**(8), 695 (2016)
41. A. Douayar, P. Prieto, G. Schmerber, K. Nouneh, R. Diaz, I. Chaki, Z. Sekkat, Investigation of the structural, optical and electrical properties of Nd-doped ZnO thin films deposited by spray pyrolysis. Eur. Phys. J **61**(1), 10304 (2013)
42. Y. Prabhu, K.V. Rao, V.S.S. Kumar, B.S. Kumari, X-ray analysis of Fe doped ZnO nanoparticles by Williamson–Hall and size-strain plot methods. Int. J. Eng. Adv. Technol. **2**, 268–274 (2013)
43. A.K. Zak, W.A. Majid, M.E. Abrishami, R. Yousefi, X-ray analysis of ZnO nanoparticles by Williamson–Hall and size–strain plot methods. Solid State Sci. **13**(1), 251–256 (2011)
44. E. Erdoğan, X-ray line-broadening study on sputtered InGaN semiconductor with evaluation of Williamson–Hall and size–strain plot methods. Indian J Phys. **93**(10), 1313–1318 (2019)
45. V.D. Mote, Y. Purushotham, B.N. Dole, Williamson–Hall analysis in estimation of lattice strain in nanometer-sized ZnO particles. J. Theor. Appl. Phys. **6**(1), 6 (2012)
46. A.R. Devi, A.J. Christy, K.D.A. Kumar, S. Valanarasu, M.S. Hamdy, K.S. Al-Namshah, H.S. Kim, Physical properties evaluation of nebulized spray pyrolysis prepared Nd doped ZnO thin films for opto-electronic applications. J. Mater. Sci. **30**(8), 7257–7267 (2019)
47. T.D. Rani, K. Tamilarasan, K. Thangaraj, E. Elamurugu, K. Ramamurthi, S. Leela, Structural and optical properties of

Nd^{3+} doped zinc oxide thin films deposited by spray pyrolysis. Optik **127**(1), 72–75 (2016)
48. S. Habashyani, A. Özmen, S. Aydogan, M. Yilmaz, An examination of correlation between characteristic and device performance of ZnO films as a function of La content. Vacuum **157**, 497–507 (2018)
49. T.P. Rao, S.G. Raj, M.S. Kumar, Effect of annealing atmosphere on structural and optical properties of Nd:ZnO thin films. Proc. Mater. Sci. **6**, 1631–1638 (2014)
50. H. Cherrad, M. Addou, M. Hssein, K. Bahedi, M. Jbilou, A. Mrigal, M. El Jouad, Theoretical and experimental investigation of structural, electronic and optical properties of neodymium doped ZnO. MATEC Web Conf **307**, 01018 (2020)